Alteration in HSP60 and HSP10 status during high fat high fructose diet induced pro-atherogenic remodeling in thoracic aorta of C57BL/6J mice

Introduction

Development of atherosclerosis is a complex multi-stage process that involves an interplay of multiple cell types including the vascular cells and the immune cells, culminating in formation of lipid-laden plaque. The onset of lesion formation is preceded by endothelial dysfunction at the predilection sites (Mudau et al., 2012). Classical atherogenic stressors induce an oxidative burst in endothelial cells (ECs) leading to reduction in production of nitric oxide (NO) that translates into reduction of vascular tone. Subsequent endothelial expression of adhesion molecules (ICAM-1, VCAM-1, E-selectin) facilitates sub-intimal recruitment of mononuclear cells initiating pro-inflammatory cascade that contributes towards overall progression of the atherogenic lesion formation (Gimbrone & Garcia-Cardena, 2016; Sitia et al., 2010). These events are also accompanied by overall structural remodeling of the vascular wall that involves degradation and reorganization of the extracellular matrix components along with cellular processes like cell proliferation and migration (van Varik et al., 2012). Thus, EC dysfunction and activation are critical events that trigger the initiation of atherosclerotic lesions and it is imperative to understand the underlying molecular mechanisms.

T-cells and monocytes are amongst the earliest infiltrators of the vascular wall during atherogenic initiation wherein monocytes differentiate into macrophages and contribute to foam cell mediated plaque formation. Interestingly, T-cells infiltration precedes the appearance of macrophages/foam cells in early lesions, whereas in the late stage of the disease the situation gets reversed with the number of foam cells exceeding that of the

lymphoid cells (Xu et al., 1990). These observations laid strong foundation for the 'auto-immune concept' of atherosclerotic initiation as the repertoire of T-cells in early lesions were identified to be auto-reactive towards heat shock protein 60 (HSP60) (Kleindienst et al., 1993; Xu et al., 1993).

HSP60 is a molecular chaperone that predominantly functions in mitochondrial protein folding and is upregulated in conditions of mitochondrial stress (Pellegrino et al., 2013). Owing to the high structural homology of HSP60 with its bacterial counterpart, pre-existing immunity against the latter fails to recognize the autologous HSP60 in stressed cells, triggering an immune cross-reaction that damages the arterial wall (Kleindienst et al., 1993). In this context, stress induced translocation of HSP60 from mitochondria to plasma membrane of ECs has been identified to be a crucial (Xu et al., 1994). It is known to activate both innate and adaptive immune system (Kleindienst et al., 1993; Mayr et al., 1999) and hence, acts as a bridge between immune cells and vascular endothelium during atherogenic initiation. Apart from surface expression, presence of soluble HSP60 in the extracellular milieu has also be found to be crucial in activating inflammatory immune reactions via toll-like receptor 4 (TLR-4) activation, thus contributing towards atherogenic progression (Kol et al., 2000; Vabulas et al., 2001). Also, the adaptive immune response (B cell activation) reported in advanced plaques have been attributed to the soluble HSP60 (Cohen-Sfady et al., 2005). Thus, the auto-antigenic role of surface expressed and soluble forms of HSP60 in early stages of atherosclerosis is known, but the significance of HSP60 upregulation in stress induced atherogenic initiation in endothelium lacks clarity.

The classical protein folding function of HSP60 in mitochondrial matrix is essentially HSP10-dependent process. Seven molecules of HSP60 together with seven molecules of

HSP10 form an enclosed chamber wherein, unfolded or misfolded proteins are folded or refolded, respectively, in the presence of ATP (Dubaquié et al., 1997; Nisemblat et al., 2015). Apart from protein folding, HSP10 has been reported to be involved in various diseases. In this regards, upregulation of HSP10 has been observed in serum of patients with auto-immune pancreatitis and fulminant type 1 diabetes (Takizawa et al., 2009). In a study with cardiomyocytes, doxorubicin induced overexpression of HSP10 and HSP60 was found to inhibit apoptosis via upregulation of B-cell lymphoma-extra large (Bcl-xl) protein (Shan et al., 2003). This indicates towards a possible role of HSP10 and HSP60 in processes apart from protein folding. Also, immunomodulatory properties of HSP10 has been reported that raise the possible involvement in atherosclerosis. However, such correlations have not been documented till date.

In this study, we had evaluated the status of HSP60 and HSP10 in vascular wall during high fat high fructose (HFHF) diet induced pro-atherogenic vascular remodeling and early atherogenic changes in endothelium in C57BL/6J mice.

Materials and methods

Experimental model: C57BL/6J male mice aged 4-6 weeks each weighing 20-22g. Particulars of animal maintenance and the ethical statement are provided in Materials and methods section.

Animal Experimentation Protocol

Experimental groups:

After 10 days acclimatization, mice were randomly divided into two groups:

1. Chow diet group (n=6, fed with laboratory chow diet) and

2. HFHF diet group (n=12, fed with high fat diet containing 35.3% fat content and 20% fructose in water).

Food intake and body weight was monitored every alternate day. After 16 weeks, mice were euthanized under mild isoflurane anesthesia and blood and thoracic aorta were collected as mentioned in Materials and methods section.

Parameters tested:

1. Serum lipid profile: TG, TC, VLDL, LDL-Chol, HDL-Chol, LDL-Chol:HDL-Chol ratio
2. Histology and morphometry
3. Elastin autofluorescence
4. Picrosirius red staining
5. Quantitative RT-PCR: HSP60, Collagen-I, Collagen-II, eNOS, VCAM-1, ICAM-1, MCP-1, HSP10, GAPDH
6. Immunoblotting: HSP60, HSP10, β-actin
7. Immunohistochemistry: HSP60, CD68

The experimental protocol for the present study is depicted in Fig. 1.1. Detailed methodology is described in materials and methods section.

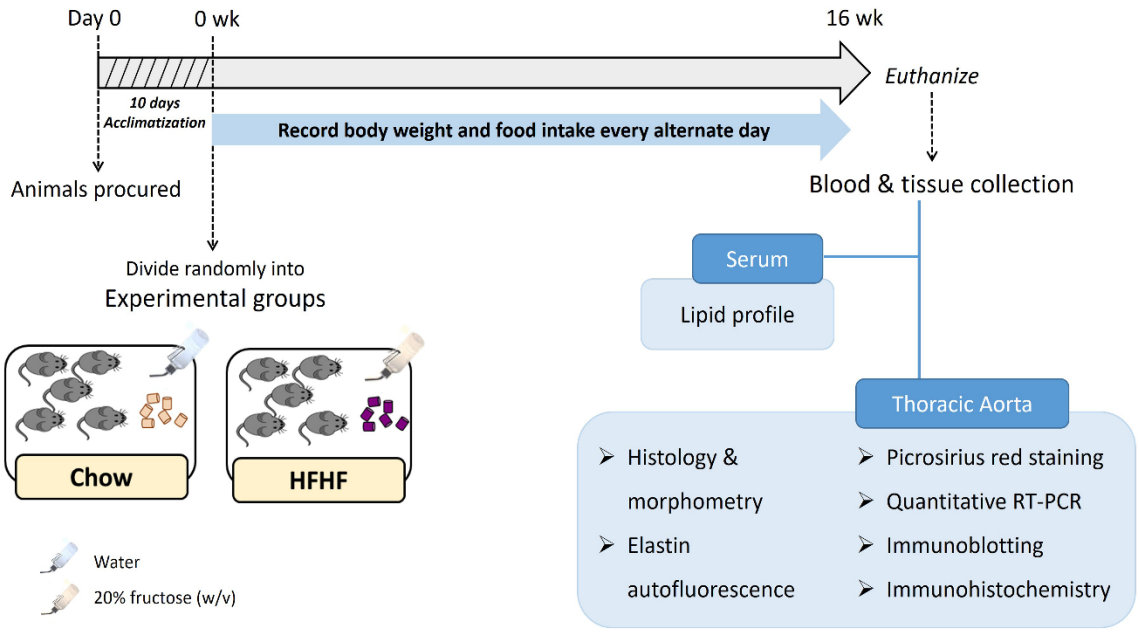

Figure 1.1: Flow chart of experimental protocol followed for studying HFHF induced atherosclerosis.

Results

HFHF diet mediated alterations in body weight, food intake and serum lipid profile

C57BL/6J mice fed with HFHF diet recorded significant increment in body weight but the food intake was significantly lower as compared to chow fed mice (Fig. 1.2). The serum levels of TG, TC, VLDL, LDL-Chol and LDL-Chol:HDL-Chol ratio were significantly elevated whereas, HDL-Chol levels were significantly lowered in HFHF diet fed mice as compared to Chow group (Fig. 1.3).

HFHF diet induces vascular remodeling in thoracic aorta

Microscopic evaluation of thoracic aorta (HXE stained; 100X & 400X) showed a significant remodeling of the intima and media of HFHF diet fed mice (Fig. 1.4a). These mice also recorded a significant increment in intima-media thickness and lumen area as compared to chow fed mice (Fig. 1.4b & c). Observations of elastin autofluorescent sections of thoracic aorta revealed marked derangement of elastin laminae (Fig. 1.5a) with significantly higher number of breaks in HFHF diet fed mice as compared to Chow group (Fig. 1.5b). Picrosirius red stained section of thoracic aorta of HFHF fed mice showed thickening in the outer collagen area (Fig. 1.6a) along with significantly elevated indices of collagen deposition (Fig. 1.6b). Also, a significant increment of ~4.8 folds in collagen I and decrement of ~0.37 folds in collagen III mRNA levels was observed in thoracic aorta of HFHF group compared to Chow group (Fig. 1.6c). Further, a significantly higher collagen-to-elastin ratio was recorded in thoracic aorta of HFHF fed mice (Fig. 1.6d).

HFHF diet induces endothelial dysfunction and activation in thoracic aorta

Endothelial nitric oxide synthase (eNOS) is an important marker of endothelial function as it mediates synthesis of NO which is a key vasodilator essential for vascular homeostasis. Herein, eNOS mRNA expression was assessed in the thoracic aorta and it was found to decrease significantly in HFHF diet fed mice as compared to chow fed mice (Fig. 1.7a). Endothelial activation and macrophage recruitment is a key atherogenic events that we assessed herein by checking the expression of MCP-1 chemokine and adhesion molecules (VCAM-1, ICAM-1). Feeding with HFHF diet resulted in significant upregulation of the said genes as compared to Chow group (Fig. 1.7b-d). Further, expression of CD68 (macrophage marker) was checked in sections of thoracic aorta and significant increase in CD68 positive areas was observed in HFHF fed mice (Fig. 1.8a & b).

HFHF diet induces HSP60 upregulation in thoracic aorta

Sections of thoracic aorta were stained with anti-HSP60 antibody that recorded a significantly higher staining in HFHF group compared to Chow group and that the intensity of HSP60 staining was much prominent in tunica intima and media (Fig. 1.9a & b). Similarly, immunoblots also recorded significant upregulation of HSP60 was observed in thoracic aorta of HFHF fed mice (Fig. 1.9c & d).

HFHF diet induces HSP10 upregulation in thoracic aorta

A significant upregulation of HSP10 mRNA (Fig. 1.10a) and protein (Fig. 1.10b & c) was observed in thoracic aorta of HFHF group as compared to Chow group.

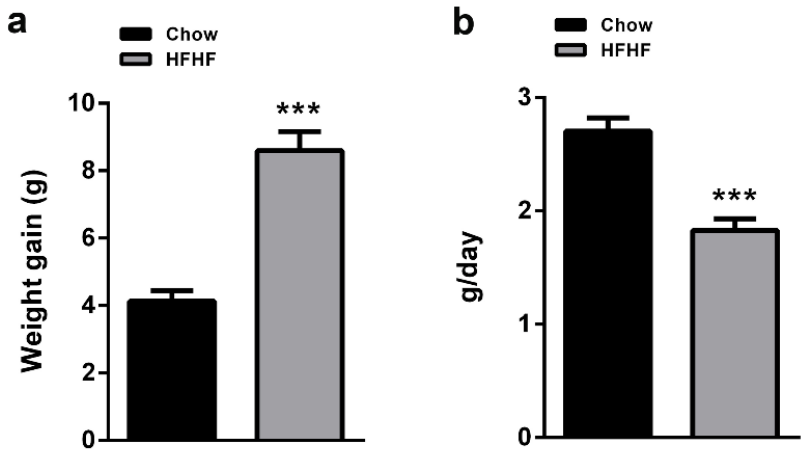

Figure 1.2: Weight gain and food intake in HFHF diet fed mice. The graphs represent (a) final weight gain per mice and (b) average food intake per mice per day in chow diet and HFHF diet fed mice (n=6 for Control, n=12 for HFHF). Data were represented as Mean ± SEM. ***p<0.001 vs Chow.

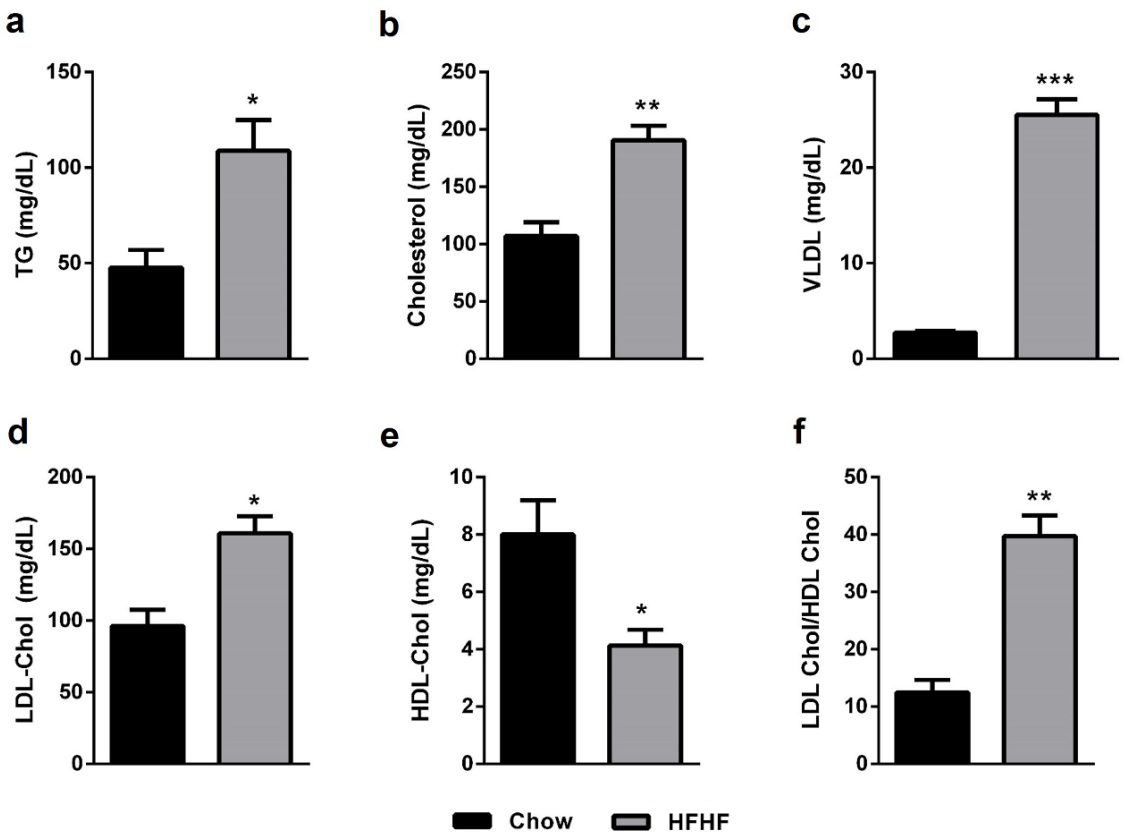

Figure 1.3: Serum lipid profile of HFHF diet fed mice. The graphs represent serum titers of (a) triglycerides (TG), (b) total cholesterol (TC), (c) very low density lipoprotein (VLDL), (d) low density lipoprotein cholesterol (LDL-Chol), (e) high density lipoprotein cholesterol (HDL-Chol) and (f) LDL-Chol/HDL-Chol ratio were assayed (n=6). Data were represented as Mean ± SEM. *p<0.05, **p<0.01, ***p<0.001 vs Chow; ns- non-significant.

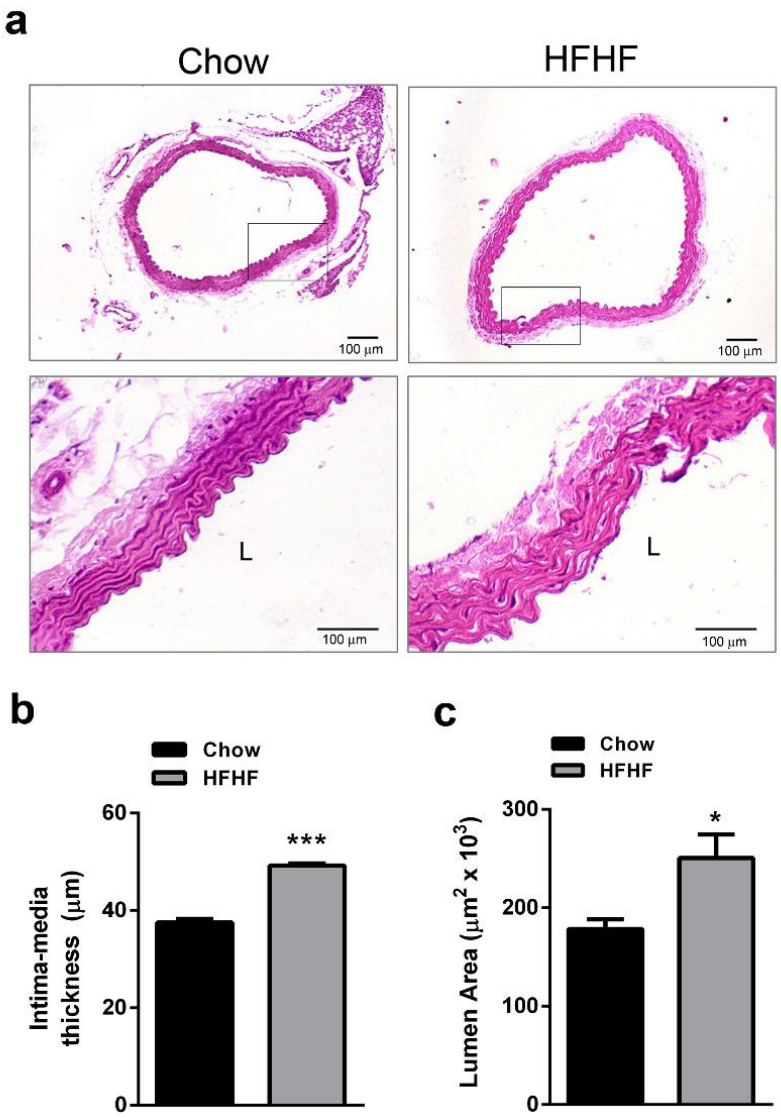

Figure 1.4: Histological and morphometric analysis of thoracic aorta of HFHF diet fed mice. Sections of thoracic aorta were stained with HXE and (a) representative images are shown. Scale bar= 100µm. The graphs represents morphometric analysis of (b) intima-media thickness (IMT) and (c) lumen area (n=6). Data were represented as Mean ± SEM. *p<0.05, ***p<0.001 vs Chow. L-Lumen.

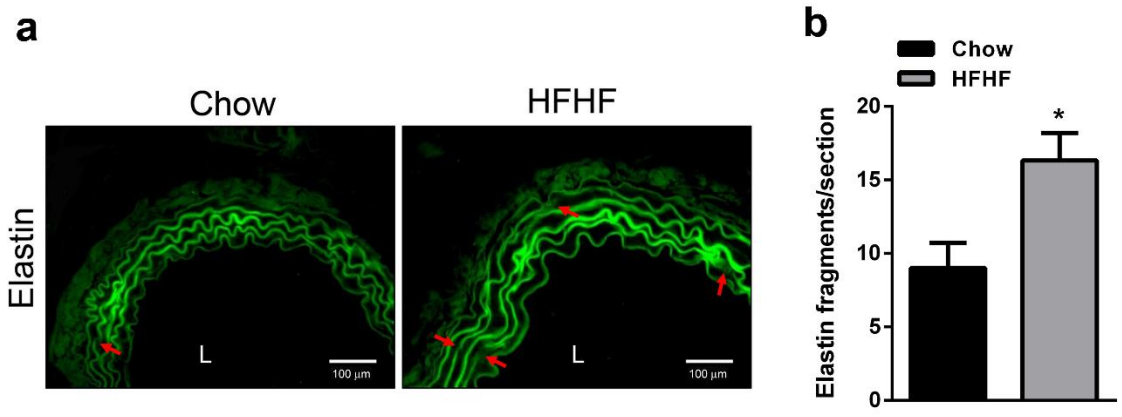

Figure 1.5: Elastin derangement in thoracic aorta of HFHF diet fed mice. Sections of thoracic aorta were subjected to assessment of (a) elastin autofluorescence (scale bar= 100µm) where red arrows indicate elastin breaks. (b) Elastin fragmentation was counted from elastin autofluorescent sections (n=6). Data were represented as Mean ± SEM. *p<0.05 vs Chow. L-Lumen.

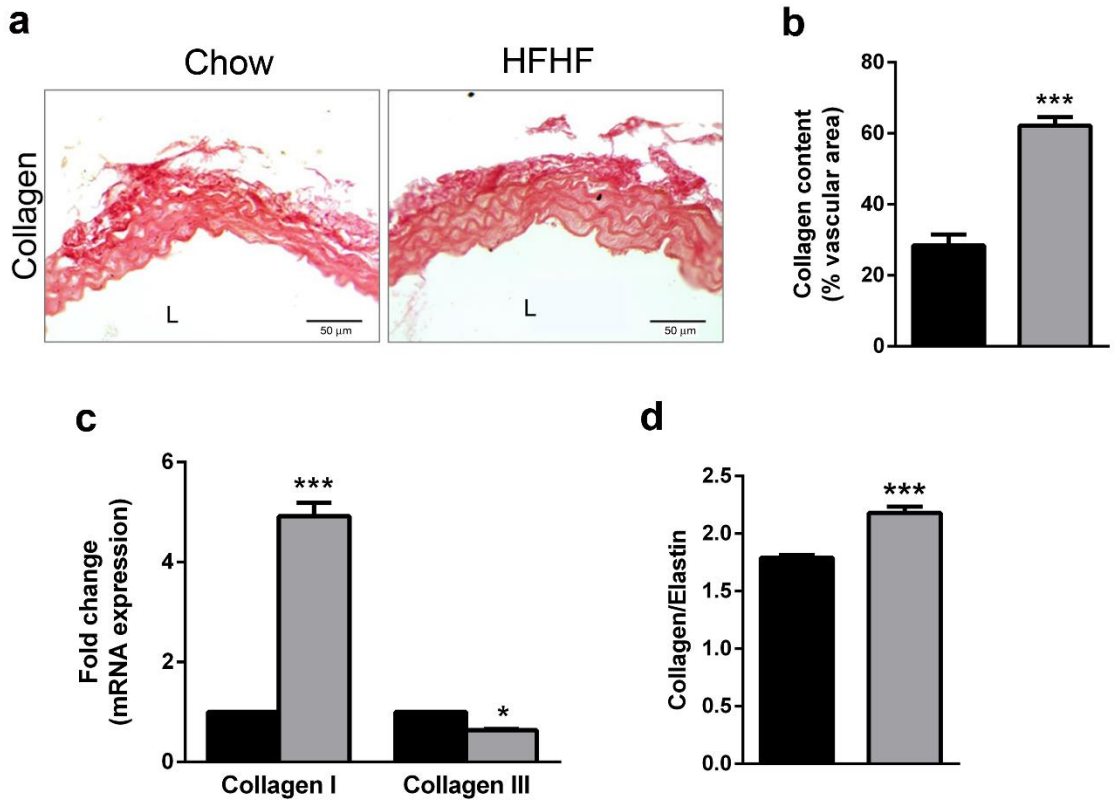

Figure 1.6: Collagen content in thoracic aorta of HFHF diet fed mice. Sections of thoracic aorta were stained with picrosirius red and (a) images were captured (Scale bar= 50µm). Quantitative analysis was carried out to determine the (b) collagen content relative to vascular area (n=6). (c) Thoracic aorta were also subjected to quantitative RT-PCR for analyzing the mRNA expression of collagen I and collagen III (n=3). (d) Collagen-to-elastin ratio (n=6) was quantified from picrosirius red stained sections as a measure of arterial stiffness. Data were represented as Mean ± SEM. *p<0.05, ***p<0.001 vs Chow. L-Lumen.

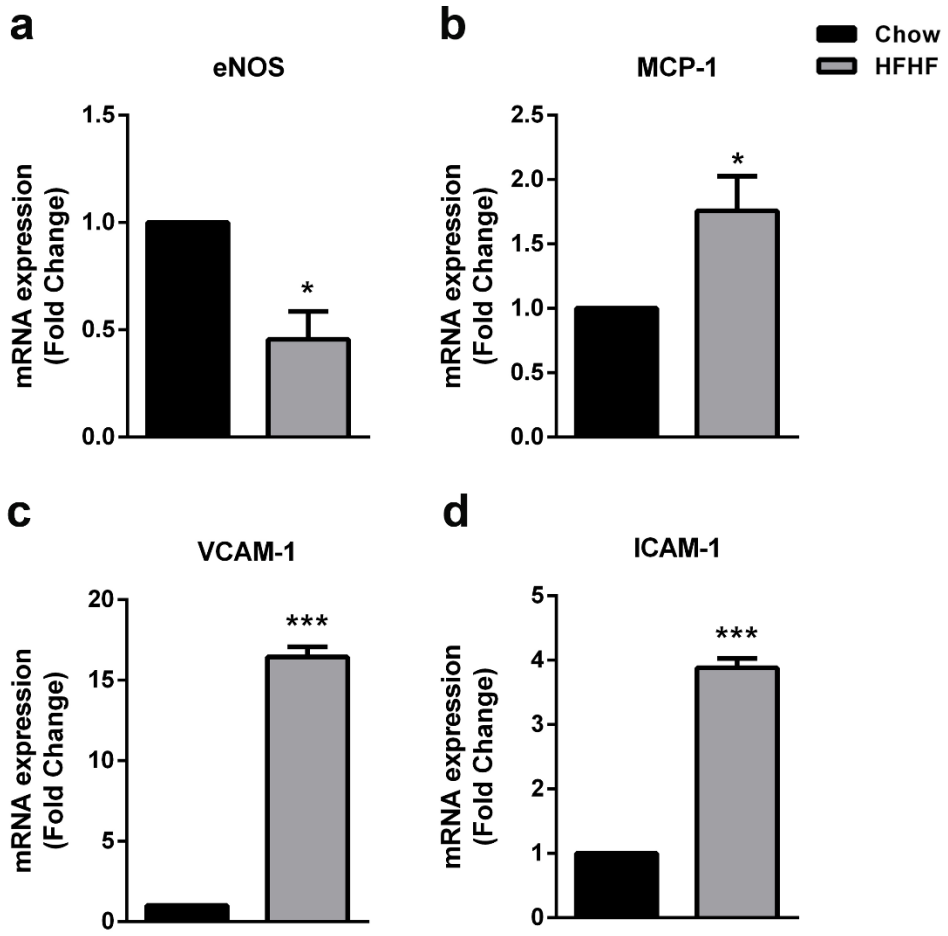

Figure 1.7: Endothelial dysfunction and activation in thoracic aorta of HFHF diet fed mice. Thoracic aorta of Chow and HFHF groups were subjected to quantitative RT-PCR for assessing mRNA expression of (a) eNOS, (b) MCP-1, (c) VCAM-1 and (d) ICAM-1. Data were expressed as Mean ± SEM (n=3). *p<0.05, ***p<0.001 vs Chow.

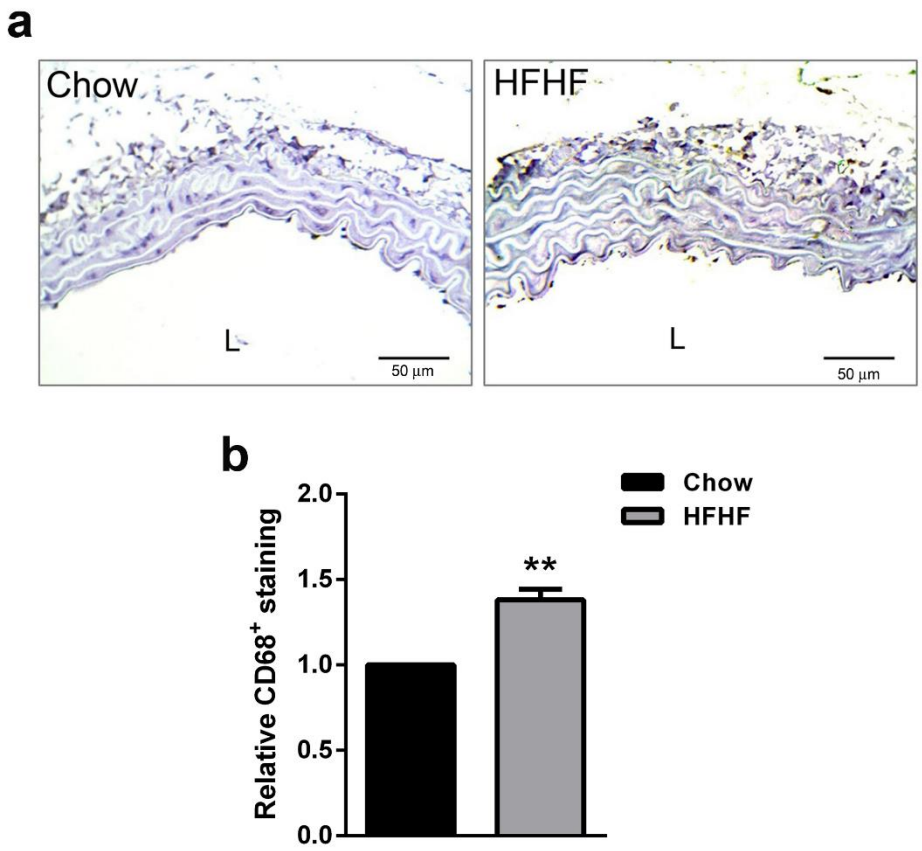

Figure 1.8: Macrophage infiltration in thoracic aorta of HFHF diet fed mice. (a) Sections of thoracic aorta were immunostained for CD68 (macrophage marker; Scale bar=50µm) and (b) positively stained area were quantified using ImageJ. Data represents Mean ± SEM (n=6). **P<0.01 vs Chow. L-Lumen.

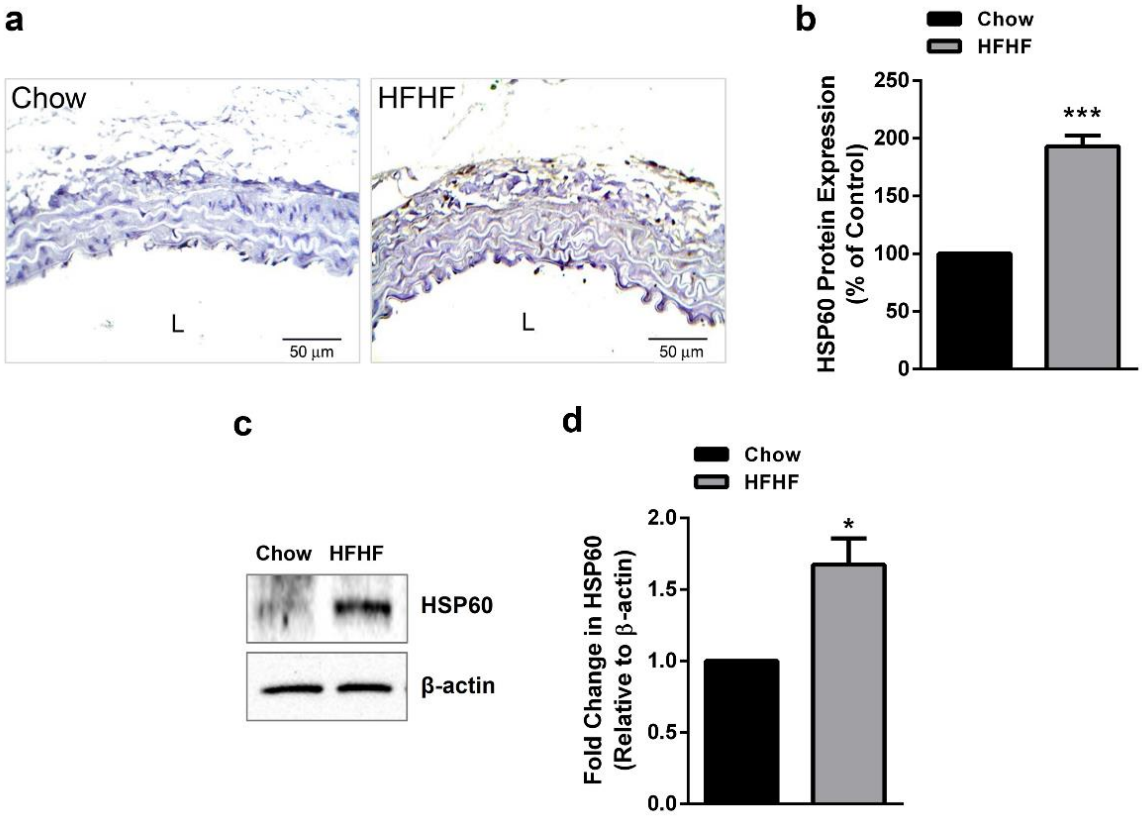

Figure 1.9: HSP60 expression in thoracic aorta of HFHF diet fed mice. (a) Sections of thoracic aorta were immunostained for HSP60 and (b) positive stained regions were quantified using ImageJ (n=6). (c) HSP60 expression was checked by immunoblotting and (d) the bands were quantified by densitometry (n=3). Data were represented as Mean ± SEM. *p<0.05, ***p<0.001 vs Chow.

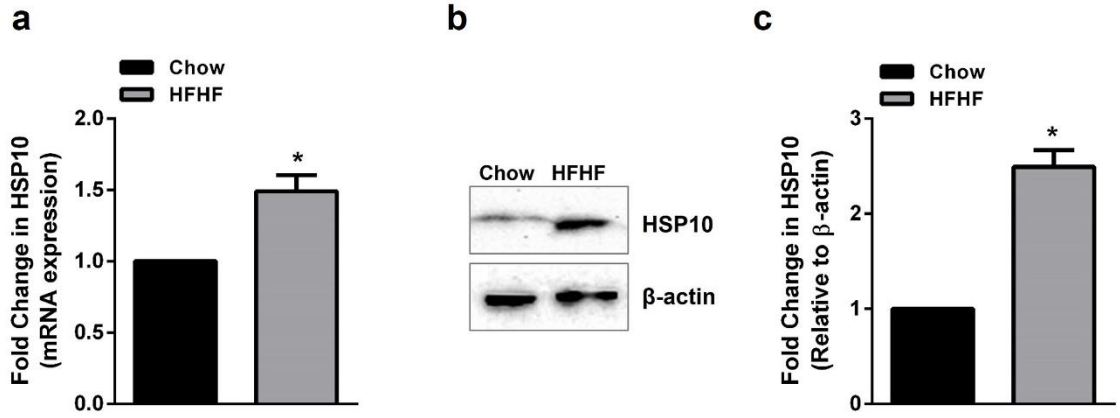

Figure 1.10: HSP10 expression in thoracic aorta of HFHF diet fed mice. HSP10 expression in thoracic aorta of Chow and HFHF groups was assessed (a) quantitative RT-PCR and (b) immunoblotting. (c) The blots were quantified by densitometry. Data were represented as Mean ± SEM (n=3). ***p<0.001 vs Chow.

Discussion

The earliest stages of atherosclerosis clearly fulfils all the postulates of N. R. Rose and E. Witebsky (Rose & Witebsky, 1956), defining atherosclerosis to be an auto-immune disease. Insights of the same have been provided by the investigations of early and late atherosclerotic lesions in humans wherein, HSP60 specific T-cell mediated immune reactions initiated the disease (Knoflach et al., 2007) and auto-antibodies to HSP60 accelerated its progression (Knoflach et al., 2005). However, endothelial dysfunction certainly precedes the formation of early lesions that are characterized by presence of auto-reactive T-cells. In the present study, we investigated the alterations in HSP60 expression during atherogenic transformation of vascular endothelium in order to establish a preliminary line of evidence for HSP60 to be the missing link between high fat high fructose (HFHF) diet induced endothelial dysfunction and pro-atherogenic vascular remodeling.

High fat diet has been known to induce metabolic alterations that correlates with perturbations in serum lipid profiles, enhanced body weight and atherogenic manifestation in C57BL/6J mice (Santana et al., 2014). Herein, feeding of HFHF diet to the same strain of mice followed a similar trend with higher body weight gain as compared to mice fed with chow diet, despite of lower feed consumption in the former. Also, the serum lipid profile of HFHF group showed a severe hyperlipidemic condition with higher LDL-Chol/HDL-Chol ratio indicating metabolic perturbation characteristic of HFHF diet (Upadhyay et al., 2018). Given the key role of LDL-cholesterol in atherosclerotic plaque formation, it can be said that the observed lipid profile in HFHF diet fed mice serves as a classical atherogenic risk factor.

Intima-media thickening is a prominent pro-atherogenic feature that is studied as one of the marker of arterial remodeling (O'Leary & Polak, 2002). Thoracic aorta of HFHF diet fed mice showed prominent hypertrophy of the vessel wall along with lumen dilation and elastin derangement indicating towards pro-atherogenic remodeling. In addition, extensive elastin fragmentation along with increased collagen deposition in the media and adventitia accounted for a higher collagen-to-elastin ratio. These changes often compromise the vascular function and distensibility increasing the arterial rigidity (Li et al., 2018).

The structural changes in arterial wall and the related functional alterations are known to be resulting from underlying endothelial dysfunction. ECs exists as a monolayer forming the intima of the vascular wall and is therefore, prone to damage by external stressors. It also plays a key role in maintenance of vascular tone by synthesizing NO, a critical vasodilator known to activate VSMC relaxation through ACE pathway (Li et al., 2018). eNOS being indispensable for NO production in ECs, it is extensively studied as an indirect measure of NO bioavailability. Herein, downregulation of eNOS mRNA expression in thoracic aorta of HFHF diet fed mice is indicative of a reduction in NO bioavailability. These observations support our claim of HFHF induced endothelial dysfunction that also contributes in increasing arterial stiffness. Other studies with high fat diet induced obesity models had also shown decreased vascular reactivity indicating endothelial dysfunction (Lang et al., 2019; Santana et al., 2014), and our results are in agreement.

During atherogenesis, endothelial dysfunction is followed by endothelial activation wherein expression of MCP-1 and adhesion molecules (ICAM-1 and VCAM-1) help in recruitment of monocytes to the sub-intimal space (van Varik et al., 2012). In our study, upregulation of MCP-1, ICAM-1 and VCAM-1 mRNAs supported the accumulation of

macrophages in thoracic aorta as depicted by CD68+ area in HFHF diet fed mice. These results mark the atherogenic transformation of endothelium that triggers the initiation of atherogenic lesion formation as reported by other groups as well (Fotis et al., 2012; Iiyama et al., 1999).

Various *in vitro* and *in vivo* studies have reported overexpression of HSP60 during atherogenic activation of endothelium (Amberger et al., 1997; Hochleitner et al., 2000; Kreutmayer et al., 2011; Kreutmayer et al., 2013; Seitz et al., 1996). Also, high fat diet induced HSP60 expression in atheromatous plaques in aortic root has been reported in BALB/c mice (Zhao et al., 2015). On the other hand, our results showed HFHF induced upregulation of HSP60 in intima and media at the earliest stage of the atherogenic initiation suggesting that HSP60 upregulation is rather an initial response of the vascular wall in response to atherogenic stressor, which in this case is hyperlipidemia. Further, the HSP60 expression in media that is majorly represented by VSMCs might explain the observed hypertrophy as HSP60 upregulation in VSMCs has been reported to induce its proliferation (Deniset et al., 2018). Also, the intimal upregulation of HSP60 correlated with endothelial dysfunction and expression of adhesion molecules indicating the existence of cross-talk between these two events in stressed ECs that needs further scrutiny.

The canonical chaperonin function of HSP60 is known to be dependent upon the presence of its co-chaperone, HSP10 (Nisemblat et al., 2015). Since HSP60 is studied extensively in atherogenic processes and we checked expression of HSP10 in thoracic aorta of HFHF fed mice. The observed upregulation of HSP10 provides preliminary evidence in support of the possibility of its role in regulating initial atherogenic processes either directly or in concert with HSP60. To the best of our knowledge, this is the first ever report of HSP10

in atherosclerosis and the same needs to be studied extensively in order to obtain a repertoire of confirmed supporting evidences.

Overall, this study provides preliminary evidence of HSP60 upregulation in endothelium to be a missing link between atherogenic transformation of endothelium and early pro-atherogenic remodeling in conditions of diet induced hyperlipidemia. The results also suggest an alteration in HSP10 expression in arterial wall as one of the consequences of hyperlipidemic stress.